Asociación Argentina
de Mecánica Computacional

Mecánica Computacional Vol XXIX, págs. 1861-1877 (artículo completo)
Eduardo Dvorkin, Marcela Goldschmit, Mario Storti (Eds.)
Buenos Aires, Argentina, 15-18 Noviembre 2010

TRANSIENT DYNAMIC STRUCTURAL ANALYSIS OF BARS AND TRUSSES USING THE GENERALIZED FINITE ELEMENT METHOD

André J. Torii and Roberto D. Machado

Programa de Pós-Graduação em Métodos Numéricos em Engenharia, Universidade Federal do Paraná, Centro Politécnico, CEP 81531-990, Curitiba, Brazil

Keywords: dynamic analysis, transient, generalized finite element, hierarchical finite element.

Abstract. The Generalized Finite Element Method (GFEM) can be viewed as a standard Finite Element Method (FEM) enriched by a family of shape functions appropriately chosen. Many applications of the GFEM can be found in literature, mostly when some information about the solution is known a priori. This paper presents the application of the GFEM to the problem of transient dynamic analysis of bars and trusses. Since the analytical solution of this problem leads, in most cases, to a trigonometric series, the enrichment used in this paper is composed of sine and cosine functions. The method of Newmark is used for the time integration procedure. The results and implementation issues are then compared to the ones obtained with a standard FEM using linear elements, and a Hierarchical Finite Element Method (HFEM) using higher order elements.

1 INTRODUCTION

Dynamic analysis of structures is an essential part of engineering mechanics (Chopra, 1995), and the application of the Finite Element Method (FEM) to this problem has been one of the most widespread approaches over the last decades (Zienkiewicz and Taylor, 1991; Bathe, 1996; Hughes, 2000). In this context, the accuracy of numerical solutions for these problems are influenced mainly by two aspects: numerical errors involved in time integration procedure; and errors involved in field quantities approximation.

The errors involved in the time integration procedure have been subject of study of many authors, but a general review is presented by Bathe (1996), Hughes (2000) and Chopra (1995). In a few words, there is a wide range of methods available for this task (i.e. Central Differences, Newmark's Method, Houbolt's Method), but once some method is chosen numerical errors can be reduced by assuming smaller time steps.

The field quantities approximations is, in general, made by some numerical method such as the FEM, the Boundary Element Method (BEM) or the Finite Differences Method (FDM). Anyway, the errors involved in this approximation depend on the form assumed for the approximation (i.e. constant, linear, quadratic) and on the number of degrees of freedom used. That is, one can reduce errors by assuming higher order approximations or by increasing the number of nodes used.

The resulting errors of dynamic analysis depend on both the time integration procedure and the field quantities approximation. Thus, these errors cannot be reduced indefinitely by improving only one of them. This can be better understood by considering the analogy presented in Fig. 1. One cannot reduce the errors of dynamic analysis directly, but can only exert indirect influence on it by reducing the errors from FEM (field quantities approximation) or by reducing the errors from the time integration procedure. However, if one assumes a poor time step (thus leaving the errors from time integration at a high level), then one cannot reduce the errors indefinitely only by improving the field approximation. The inverse situation is also true. The only option to reduce the resulting error from dynamic analysis to a very low level is to reduce both the errors from the time integration procedure and the field approximation. This work is concerned with the reduction of errors from field approximation, by using an enriched version of the FEM called Generalized Finite Element Method (GFEM) (Babuska et al., 2004; Strouboulis et al., 2001; Arndt, 2009; Ardnt et al., 2010).

In order to improve the FEM approximation one can increase the number of degrees of freedom (i.e. increase the number of elements and nodes) and/or improve the approximation given by each finite element (i.e. increase the order of the polynomial used). In most situations it has been observed that increasing the order of the polynomials used leads to better results than simply increasing the number of nodes (Zienkiewicz and Taylor, 1991; Bathe, 1996; Hughes, 2000). However, it is difficult to formulate standard finite elements of very high order, since each time a new polynomials is included in the approximation all the polynomials used must be rewritten. In order to avoid this difficulty, some authors presented polynomials basis that are hierachical. That is, each time a new polynomial is included in the approximation the other polynomials remain the same. This leads to the Hierachical Finite Element Method (HFEM), that has been successfully applied to many problems involving higer order finite elements (Solín et al., 2004).

Here we propose an hierachical formulation that is based on the GFEM (Babuska et al., 2004; Strouboulis et al., 2001; Arndt, 2009; Ardnt et al., 2010) and the Partition of Unity (PU) (Melenk and Babuska, 1996) approaches. In this case, the FEM approximation is enriched by

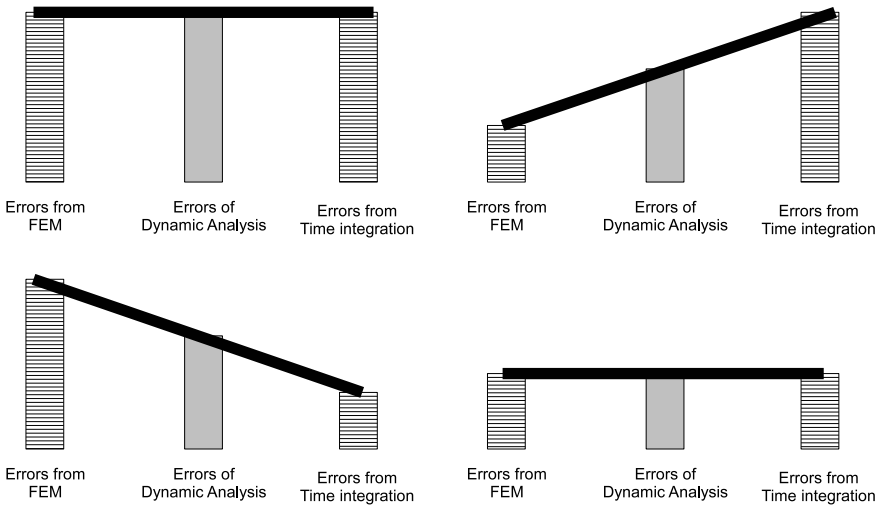

Figure 1: The relation of the errors involved in dynamic analysis.

shape functions that are obtained applying the PU approach to sine and cossine functions, thus giving a GFEM. This approach has already been successfully applied to the modal analysis of bars and trusses by Arndt (2009) and Ardnt et al. (2010), but now we apply it to dynamic analysis using direct time integration procedures (by using Newmark's method). A detailed survey of the literature regarding the subject is presented by Arndt (2009).

2 GENERALIZED FINITE ELEMENTS FORMULATION

In a standard Finite Elements formulation, the displacements inside a given finite element are approximated by (Zienkiewicz and Taylor, 1991; Reddy, 1998)

$$u_h(\xi) = \sum_{i=1}^{n} u_i N_i(\xi), \tag{1}$$

where u_i are nodal degrees of freedom, $N_i(\xi)$ are the shape functions and ξ is the position inside the domain of a given finite element.

However, the approximation given by Eq. (1) can be enriched by using

$$u_h(\xi) = \sum_{i=1}^{n} u_i N_i(\xi) + \sum_{i=1}^{m} c_i \phi_i(\xi), \tag{2}$$

where $\phi_i(\xi)$ are enrichment functions and c_i are the associated degrees of freedom.

According to Melenk and Babuska (1996), Babuska et al. (2004) and Strouboulis et al. (2001), the enrichment functions $\phi_i(\xi)$ can be obtained using a Partition of Unity (PU) approach, where the shape functions $N_i(\xi)$ from standard FEM form a PU. However, as can be seen from Fig. 2, the PU for the FEM is actually given by the "hat" function defined over two elements. In Fig. 2 the finite elements are tagged as el. 1, el. 2, etc. The PUs are tagged as $\eta_{\Omega 1}$, $\eta_{\Omega 2}$, etc. Note that each PU is defined over a domain Ω and that the domains Ω for which the PUs are defined are actually superposed. Actually, each PU is, in general, defined over two finite elements. The enrichment functions are then given by the multiplication of the PUs by basis functions chosen appropriately.

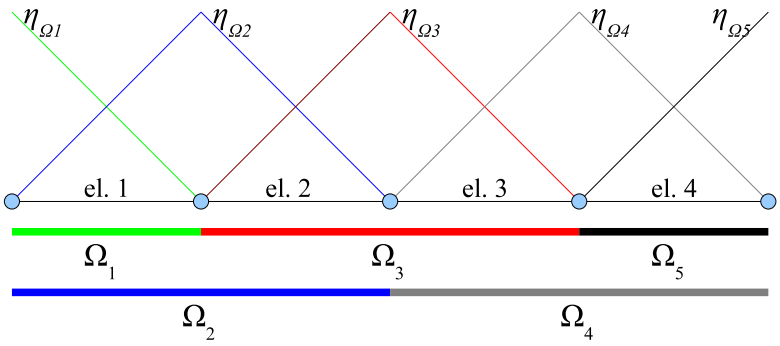

Figure 2: The Partition of Unity for a unidimensional finite element mesh.

The procedure described here for obtaining the enrichment functions is that proposed by Arndt (2009) and Ardnt et al. (2010), and leads to a Generalized Finite Element Method (GFEM) formulation. For a support Ω defined over two finite elements the PU can be defined as

$$\eta(\xi) = \begin{cases} \xi & \text{if } \xi < 1, \\ 2 - \xi & \text{if } \xi \geq 2, \end{cases} \tag{3}$$

where ξ is the local coordinate inside the support defined by two finite elements $\xi = [0, 2]$. This PU is presented in Fig. 3.

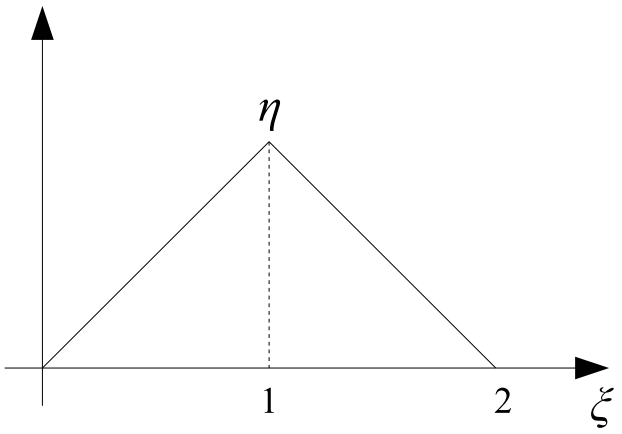

Figure 3: The Partition of unity for a support Ω defined by two finite elements.

The basis functions $\gamma(\xi)$ are assumed here to be given by

$$X = \text{span}\left\{1, \sin\left(n\xi\pi\right), \cos\left(n(\xi - 1)\pi\right) - 1, ...\right\}, \tag{4}$$

where n is an integer. The trigonometric basis functions are shown in Fig. 4 for $n = 1$. The reason behind this choice is described in details by Arndt (2009) and Ardnt et al. (2010).

An arbitrary finite element is defined by the superposition of two supports (Arndt, 2009; Ardnt et al., 2010), as can be seen in Fig. 2. Note that the element 1 is defined in the intersection between Ω_1 and Ω_2. Consequently, the displacement in this element is approximated by the PU

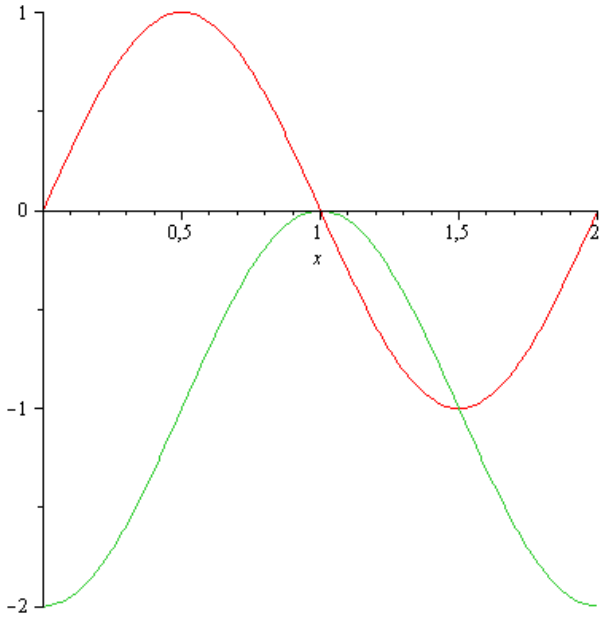

Figure 4: Basis functions for $n = 1$ on the support defined by two finite elements.

$\eta_{\Omega 1}$ multiplied by the basis functions on the support Ω_1 plus the PU $\eta_{\Omega 2}$ multiplied by the basis functions on the support Ω_2.

As can be verified by the reader, this gives the following approximation on an arbitrary finite element defined on the local coordinates $\xi = [0, 1]$ (Arndt, 2009; Ardnt et al., 2010):

$$u_h(\xi) = u_1\eta_1(\xi)+u_2\eta_2(\xi)+\sum_{i=1}^{m}\left\{c_{1i}\eta_1(\xi)\gamma_{1i}(\xi) + c_{2i}\eta_1(\xi)\gamma_{2i}(\xi) + c_{3i}\eta_2(\xi)\gamma_{3i}(\xi) + c_{4i}\eta_2(\xi)\gamma_{4i}(\xi)\right\}, \tag{5}$$

where

$$\begin{array}{l} \eta_1(\xi) = 1 - \xi \\ \eta_2(\xi) = \xi \\ \gamma_{1i}(\xi) = \sin(i\pi\xi) \\ \gamma_{2i}(\xi) = \cos(i\pi\xi) - 1 \\ \gamma_{3i}(\xi) = \sin(i\pi(\xi - 1)) \\ \gamma_{4i}(\xi) = \cos(i\pi(\xi - 1)) - 1 \end{array}, \tag{6}$$

u_1 and u_2 are nodal degrees of freedom, c_{ji} are the degrees of freedom related to the enrichment functions and m is the level of enrichment used. The functions from Eq. (6) are presented in Fig. 5, for $m = 1$.

At this point it is interesting to discuss the role of the shape functions, the basis functions and the PUs. The functions $\phi(\xi)$ are shape functions used for the enrichment. Until here we separate the shape functions in two classes: the nodal shape functions from standard FEM $N(\xi)$; and the enrichment shape functions $\phi(\xi)$. The enrichment shape functions $\phi(\xi)$ are given by the multiplication of the basis functions $\gamma(\xi)$ by the PUs $\eta(\xi)$.

The basis functions $\gamma(\xi)$ are chosen in order to incorporate some information that is known a priori, that is a general rule from the GFEM (Babuska et al., 2004; Strouboulis et al., 2001;

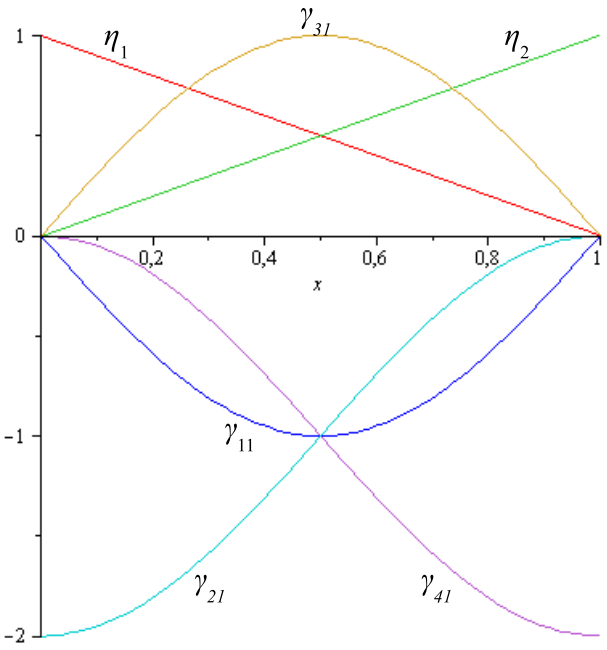

Figure 5: The functions η and γ for $m = 1$.

Arndt, 2009; Ardnt et al., 2010). Here we chose trigonometric functions as basis functions since we know that the analytical solution of the problem leads to this type of function. Besides, the basis functions used here already produced good results for modal analysis, as discussed by Arndt (2009) and Ardnt et al. (2010).

Finally, the PUs $\eta(\xi)$ can be taken as the shape functions $N(\xi)$, since summation of all the shape functions from standard FEM always result in unity. However, we still call the PUs $\eta(\xi)$ in order to emphasize that these functions are taking the role of a PU and not the role of a shape function.

Assuming one level of enrichment, that is $m = 1$, the resulting shape functions can be rewritten as

$$\begin{aligned}
\psi_1(\xi) &= 1 - \xi \\
\psi_2(\xi) &= \xi \\
\psi_3(\xi) &= (1 - \xi)(\sin(\pi\xi)) \\
\psi_4(\xi) &= (1 - \xi)(\cos(\pi\xi) - 1) \\
\psi_5(\xi) &= \xi(\sin(\pi(\xi - 1))) \\
\psi_6(\xi) &= \xi(\cos(\pi(\xi - 1)) - 1)
\end{aligned} \tag{7}$$

and the approximation inside a given finite element can be written as

$$u_h(\xi) = u_1\psi_1(\xi) + u_2\psi_2(\xi) + c_1\psi_3(\xi) + c_2\psi_4(\xi) + c_3\psi_5(\xi) + c_4\psi_6(\xi), \tag{8}$$

where ψ are the shape functions (either the ones from standard FEM N and the enrichment ones ϕ), u are nodal degrees of freedom and c are field degrees of freedom. The shape functions from Eq. (7) are shown in Fig. 6. Note that we now denote all the shape function by ψ, in order to emphasize that once all the shape functions are obtained they are all treated in the same way. That is, we now apply the standard procedure of the FEM for all the shape functions ψ. In this

context it is clear that the main difference between the FEM and the GFEM lies in the way that the shape functions are obtained.

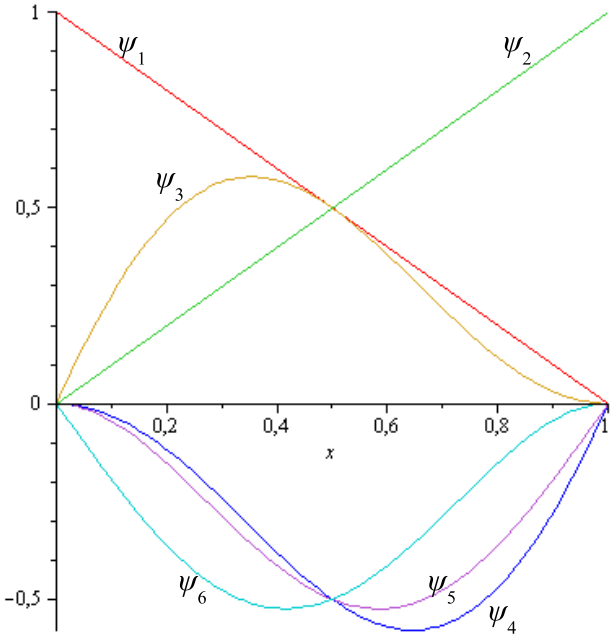

Figure 6: The shape functions for one enrichment level of the GFEM.

Assuming Eq. (8) as the displacement approximation and that the cross section area A and the Young Modulus E are constant within a given element, the stiffness and mass matrices can be obtained using the same procedure that is standard for the FEM. That is, we substitute the shape functions and its derivatives on integral expressions that are obtained by the virtual work principle or weighted residuals, as described by Bathe (1996).

For the finite element using Eq. (8) as displacement approximations we have

$$\mathbf{k} = \frac{EA}{L}\begin{bmatrix} 1 & -1 & 0 & 0 & 0 & 0 \\ . & 1 & 0 & 0 & 0 & 0 \\ . & . & \frac{3+2\pi^2}{12} & \frac{3-\pi^2}{12} & -\frac{\pi}{4} & -\frac{\pi}{2} \\ . & . & . & \frac{3+2\pi^2}{12} & \frac{\pi}{2} & \frac{\pi}{4} \\ . & . & . & . & \frac{-3+2\pi^2}{12} & \frac{21-\pi^2}{12} \\ . & . & . & . & . & \frac{-3+2\pi^2}{12} \end{bmatrix} \tag{9}$$

and

$$\mathbf{m} = \rho AL\begin{bmatrix} \frac{1}{3} & \frac{1}{6} & \frac{\pi^2-4}{\pi^3} & -\frac{4}{\pi^3} & -\frac{\pi^2-6}{3\pi^2} & -\frac{1}{6} \\ . & \frac{1}{3} & \frac{4}{\pi^3} & -\frac{\pi^2-4}{\pi^3} & -\frac{1}{6} & -\frac{\pi^2-6}{3\pi^2} \\ . & . & \frac{2\pi^2-3}{12\pi^2} & -\frac{\pi^2+3}{12\pi^2} & -\frac{3\pi^2-16}{4\pi^3} & -\frac{4}{\pi^3} \\ . & . & . & \frac{2\pi^2-3}{12\pi^2} & \frac{4}{\pi^3} & \frac{3\pi^2-16}{4\pi^3} \\ . & . & . & . & \frac{2\pi^2-15}{4\pi^2} & \frac{\pi^2+3}{12\pi^2} \\ . & . & . & . & . & \frac{2\pi^2-15}{4\pi^2} \end{bmatrix}, \tag{10}$$

that are both symmetric matrices.

3 HIERARCHICAL FINITE ELEMENTS FORMULATION

The Hierarchical Finite Element Method (HFEM) formulation proposed here uses Lobatto polynomials as described by Solín et al. (2004). In this case, the shape functions are given by

$$\begin{array}{l}\psi_1(\xi) = 1-\xi \\ \psi_2(\xi) = \xi \\ \psi_3(\xi) = \frac{1}{4}\sqrt{6}((2\xi-1)^2-1) \\ \psi_4(\xi) = \frac{1}{4}\sqrt{10}((2\xi-1)^2-1)(2\xi-1) \\ \psi_5(\xi) = \frac{1}{16}\sqrt{14}((2\xi-1)^2-1)(5(2\xi-1)^2-1) \\ \psi_6(\xi) = \frac{3}{16}\sqrt{2}((2\xi-1)^2-1)(7(2\xi-1)^2-3)(2\xi-1)\end{array} , \tag{11}$$

that are presented in Fig. 7.

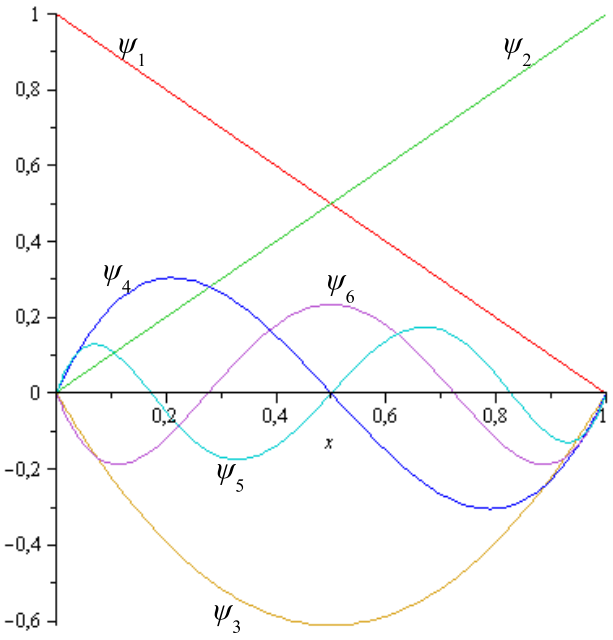

Figure 7: The shape functions for the HFEM using Lobatto polynomials.

Using Eq. (11) the stiffness matrix and the mass matrix (Bathe, 1996) for a finite element become

$$\mathbf{k} = \frac{EA}{L}\begin{bmatrix} 1 & -1 & 0 & 0 & 0 & 0 \\ . & 1 & 0 & 0 & 0 & 0 \\ . & . & 2 & 0 & 0 & 0 \\ . & . & . & 2 & 0 & 0 \\ . & . & . & . & 2 & 0 \\ . & . & . & . & . & 2 \end{bmatrix} \tag{12}$$

and

$$\mathbf{m} = \rho AL \begin{bmatrix} \frac{1}{3} & \frac{1}{6} & -\frac{\sqrt{6}}{12} & \frac{\sqrt{10}}{60} & 0 & 0 \\ \cdot & \frac{1}{3} & -\frac{\sqrt{6}}{12} & -\frac{\sqrt{10}}{60} & 0 & 0 \\ \cdot & \cdot & \frac{1}{5} & 0 & -\frac{\sqrt{84}}{420} & 0 \\ \cdot & \cdot & \cdot & \frac{1}{21} & 0 & -\frac{\sqrt{20}}{420} \\ \cdot & \cdot & \cdot & \cdot & \frac{1}{45} & 0 \\ \cdot & \cdot & \cdot & \cdot & \cdot & \frac{1}{77} \end{bmatrix}, \tag{13}$$

that are both symmetric matrices.

4 TRUSS STRUCTURES

In the previous sections we have presented the stiffness and mass matrices for the GFEM and HFEM of a bar finite element. In order to obtain the equations for a truss finite element, that can be oriented in an arbitrary direction in space, it is necessary to apply some coordinate transformation rule (Bathe, 1996; Zienkiewicz and Taylor, 1991).

For a linear finite element the following coordinate transformation hold (Bathe, 1996):

$$\begin{bmatrix} u_1' \\ u_2' \end{bmatrix} = \begin{bmatrix} \cos\theta & \sin\theta & 0 & 0 \\ 0 & 0 & \cos\theta & \sin\theta \end{bmatrix} \begin{bmatrix} u_1 \\ v_1 \\ u_2 \\ v_2 \end{bmatrix}, \tag{14}$$

where u' are the nodal displacements in local coordinates, u and v are the horizontal and vertical nodal displacements in global coordinates and θ is the angle of inclination of the truss element.

Note that according to Fig. 6 and 7, the nodal degrees of freedom for both the GFEM and the HFEM formulation are not influenced by the field degrees of freedom. Consequently, the coordinate transformation for the GFEM and the HFEM described previously can be written as (Arndt, 2009; Ardnt et al., 2010)

$$\begin{bmatrix} u_1' \\ u_2' \\ c_1' \\ c_2' \\ c_3' \\ c_4' \end{bmatrix} = \begin{bmatrix} \cos\theta & \sin\theta & 0 & 0 & 0 & 0 & 0 & 0 \\ 0 & 0 & \cos\theta & \sin\theta & 0 & 0 & 0 & 0 \\ 0 & 0 & 0 & 0 & 1 & 0 & 0 & 0 \\ 0 & 0 & 0 & 0 & 0 & 1 & 0 & 0 \\ 0 & 0 & 0 & 0 & 0 & 0 & 1 & 0 \\ 0 & 0 & 0 & 0 & 0 & 0 & 0 & 1 \end{bmatrix} \begin{bmatrix} u_1 \\ v_1 \\ u_2 \\ v_2 \\ c_1 \\ c_2 \\ c_3 \\ c_4 \end{bmatrix}, \tag{15}$$

that is, the field degrees of freedom in local coordinates c' are the same as the field degrees of field in global coordinates c, since they do not "act" on the nodes.

5 ERROR EVALUATION

One way of evaluating the error between the analytical solution $u(x,t)$ and the numerical solution $u_h(x,t)$ for a given position of the bar $x = x_0$ in the time interval $[t_0, t]$ would be to

evaluate the integral

$$e = \int_{t_0}^{t} |u(x_0, t) - u_h(x_0, t)| dt, \tag{16}$$

where $x = x_0$ is taken as a constant since the error is evaluated for a fixed position of the bar, u is the analytical solutions and u_h is the approximated solution.

Equation Eq. (16) could be used as an error estimate of the time integration procedure in a given position of the bar. However, it is not efficient to use Eq. (16) in practice since the numerical results are given as discrete points in time.

However, an approximation for Eq. (16) can be written as

$$e \approx \sum_{i=1}^{n} \Delta t |\Delta u^{(i)}| = \sum_{i=1}^{n} \Delta t |u^{(i)} - u_h^{(i)}|, \tag{17}$$

where n is the number of time steps, $u^{(i)}$ is the analytical solution at time step (i) for $x = x_0$, $u_h^{(i)}$ is the numerical solution at the time step (i) for $x = x_0$, and Δt is the time interval.

The error estimate given by Eq. (17) is pictured in Fig. 8. The integral from Eq. (16) for a given time interval $\left[t^{(i-1)}, t^{(i)}\right]$, is approximated by the product between Δt and $\Delta u^{(i)}$. This error estimate can be computed efficiently since it deals with vector quantities and thus the computational effort involved is small.

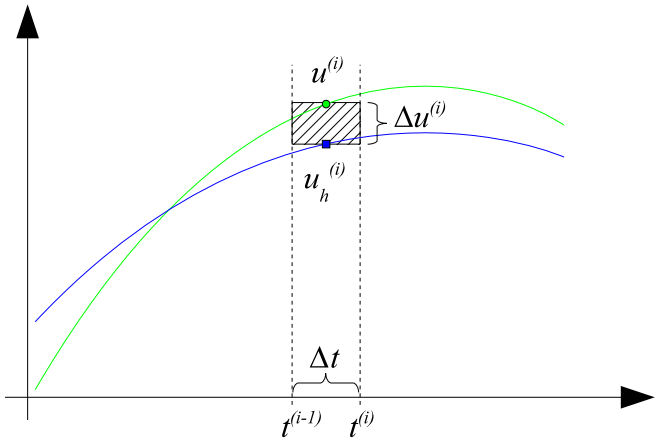

Figure 8: Error estimate for the time integration procedure.

A generalization of Eq. (16) can be written by using the definition of the internal product between two function (Kreyszig, 1978; Reddy, 1998). This gives

$$e(u, u_h) = (u - u_h, \phi)_{L^p} = \left| \int_{t_0}^{t} |u - u_h|^p |\phi|^p dt \right|^{\frac{1}{p}}, \tag{18}$$

where u and u_h are functions of t for a given $x = x_0$ and ϕ is a weight function. That is, the error can be evaluated by taking the internal product of the difference between the analytical and numerical solutions by some weight function ϕ.

In Eq. (16) we assumed $p = 1$ and $\phi = 1$, and thus Eq. (16) is a particular case of Eq. (18). However, Eq. (18) can lead to other useful error estimates. In order to see this, suppose that the weight function ϕ is actually taken as the analytical solution u. In this case, the difference

between the analytical and the numerical solution $|u - u_h|$ that appear in Eq. (18) is multiplied by the analytical solution itself, and we get

$$e(u, u_h) = (u - u_h, u)_{L^p} = \left| \int_{t_0}^{t} |u - u_h|^p |u|^p dt \right|^{\frac{1}{p}}. \tag{19}$$

From Eq. (19) we note that differences $u - u_h$ will contribute more to the error when is $|u|$ is bigger. Consequently, errors in displacements peaks will be more important than errors for small displacements. That is, Eq. (19) can be used when one wants to compare the performance of the algorithm to reproduce displacement peaks.

When p is increased from 1 to a very big number in Eq. (18), bigger differences $u - u_h$ will prevail over small ones and we get

$$e(u, u_h) = (u - u_h, \phi)_{L^\infty} = \max\left(|u - u_h|\phi\right), \tag{20}$$

when $p \to \infty$.

Note that when we take $p = 1$ both bigger smaller differences Δu will have the same importance for the error estimate. However, when we take $p = 5$, for example, bigger differences Δu will prevail over the small ones. That is, p can be modified in order to tune the importance of bigger differences $u - u_h$ over smaller ones.

As occurs for Eq. (16), the errors estimates given by Eq. (18), Eq. (19) and Eq. (20) are difficult to evaluate in practice. However, applying the same reasoning used for obtaining Eq. (17), an approximation for Eq. (18) can be written as

$$e(u, u_h) \approx \left[\sum_{i=1}^{n} \Delta t \left(|\Delta u^{(i)}||\phi^{(i)}| \right)^p \right]^{\frac{1}{p}} = \left[\sum_{i=1}^{n} \Delta t \left(|u^{(i)} - u_h^{(i)}||\phi^{(i)}| \right)^p \right]^{\frac{1}{p}}, \tag{21}$$

that is a p vector internal product between the vectors given by $|\Delta u^{(i)}|$ and ϕ, where each component i is evaluated in the time $t^{(i)}$. Note that the step from Eq. (18) to Eq. (21) is taken by going from the internal product between two functions to the internal product between two vectors. In this context, the vectors that appear in Eq. (21) are analogue the functions that appear in Eq. (18).

In this paper we adopt two error estimates, by taking the weight function as $\phi = 1$ and $\phi = u$. Besides, p is take equal to 1. The expressions for both these errors estimates can be obtained from Eq. (21) as

$$e_g \approx \sum_{i=1}^{n} \Delta t |u^{(i)} - u_h^{(i)}| \tag{22}$$

and

$$e_p \approx \sum_{i=1}^{n} \Delta t |u^{(i)} - u_h^{(i)}||u^{(i)}|, \tag{23}$$

where e_g is a general estimate and e_p is an error estimate aimed for peak displacements.

6 NUMERICAL RESULTS

6.1 First example: bar subjected to initial displacement

The first example is that of a bar subjected only to an initial displacement, as presented in Fig. 9. The bar has $E = 1$, $A = 1$, $\rho = 1$, $L = 1$ and is fixed at both ends. The initial displacement is as presented in Fig. 9, where the maximum displacement u_{max} is prescribed at the middle of the bar. Finally, there is no force acting on the bar. This problem can be solved analytically by separation of variables (Kreyszig, 2006).

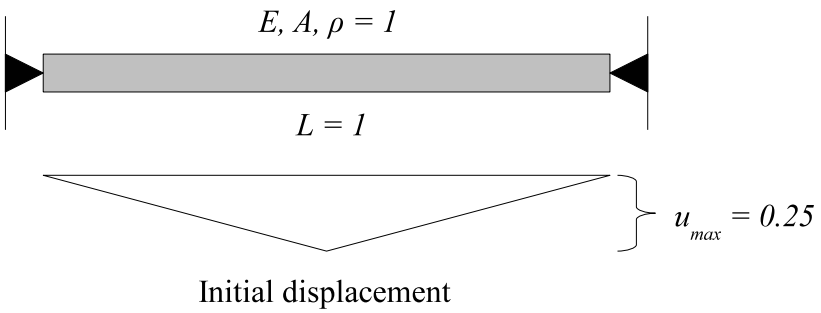

Figure 9: Bar fixed at both ends and its initial displacement.

The displacement at the middle of the bar obtained using FEM with linear elements, GFEM and HFEM is presented in Fig. 10. All analyses were made using a time step $\Delta t = 0.003125$. Besides, the analyses were made using 21 and 41 degrees of freedom. The errors e_g and e_p are presented in Tab. 1. In Fig. 10 the results for 41 degrees of freedom are not presented in order to summarize the results.

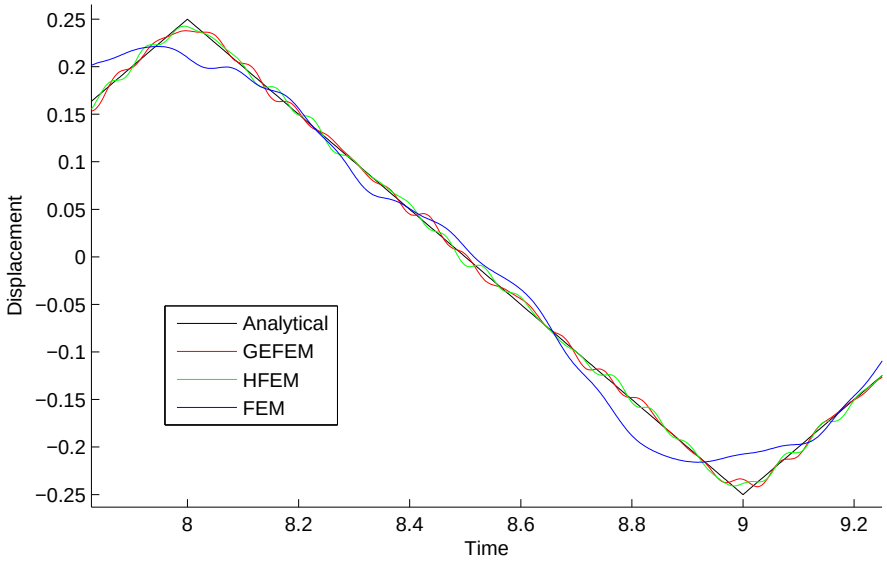

Figure 10: Analytical and numerical results at the middle of the bar for the first example using 21 degrees of freedom.

Error	GFEM21	HFEM21	FEM21	GFEM41	HFEM41	FEM41
e_p	0.0045	0.0045	0.0150	0.0019	0.0019	0.0072
e_g	0.0340	0.0343	0.1020	0.0139	0.0140	0.0454

Table 1: Errors for the first example.

From this analysis it can be seen that both the HFEM and the GFEM gave better results than the FEM with linear elements. Besides, the results of the HFEM and the GFEM are similar and it can not be concluded which one performed better in this example.

An interesting result can be obtained by evaluating the relation between the errors obtained with the FEM and the GFEM. For 21 degrees of freedom, this relation for errors e_g is equal to 3.00, while for errors e_p the same relation gives 3.33. That is, the FEM appears to give worse results according to the error estimate aimed for peak displacements e_p than for the error estimate e_g. The same behavior is observed when this relation is made for the results obtained with 41 degrees of freedom. In this case, the relation between the errors is 3.27 and 3.79 for e_g and e_p respectively. Thus, it seems that the errors given by the FEM formulation are severely influenced by its inability to represent peak displacements.

6.2 Second example: bar subjected to harmonic force

This is example is that of a bar with zero initial displacements but subjected to a time dependent force $F(t)$ applied to the left end, as shown in Fig. 11. The force is given by

$$F(t) = f \sin(\omega t), \tag{24}$$

where f is the magnitude of the force and ω is the frequency of the force.

This problem can be solved using the separation of variables for non homogeneous boundary conditions (Pinchover and Rubinstein, 2005) and its analytical solution for a bar of length $L = 1$ is

$$u(x,t) = fx \sin(\omega t) + f \sum_{i=1}^{m} \left\{ \sin(k_n x)[C_n \sin(k_n c t) + B_n(t)] \right\}, \tag{25}$$

where

$$C_n = \frac{A_n \omega}{k_n c}, \tag{26}$$

$$B_n(t) = \frac{A_n \omega^2 \sin(\omega t)}{c^2 k_n^2 - \omega^2} - \frac{A_n \omega^3 \sin(k_n c t)}{c^3 k_n^3 - c k_n \omega^2}, \tag{27}$$

$$A_n = -\frac{2[k_n \cos(k_n) - \sin(k_n)]}{k_n^2}, \tag{28}$$

$$k_n = \pi \left(n - \frac{1}{2} \right). \tag{29}$$

For this example two cases are studied, by taking $\omega = 10$ and $\omega = 30$. Besides, the magnitude of the harmonic force is $f = 1$. For $\omega = 10$ the time step is $\Delta t = 0.0015625$ while for $\omega = 30$ the time step is reduced to $\Delta t = 0.00078125$. The analyses were made using 21 and 41 degrees of freedom. The displacement at the middle of the bar for $\omega = 10$ is presented in Fig.

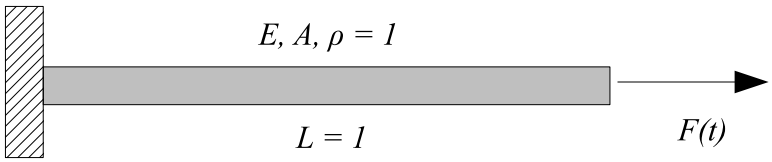

Figure 11: Bar fixed at one end subjected to a time dependent force.

12, and for $\omega = 30$ is presented in Fig. 13 where the numbers after the name of the formulations indicate the number of degrees of freedom used. The errors are presented in Tab. 2 and Tab. 3.

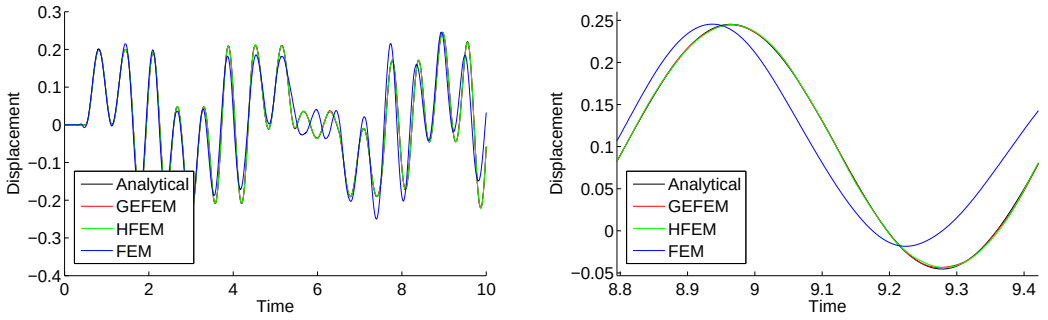

Figure 12: Analytical and numerical results for $\omega = 10$ at the middle of the bar for using 21 degrees of freedom.

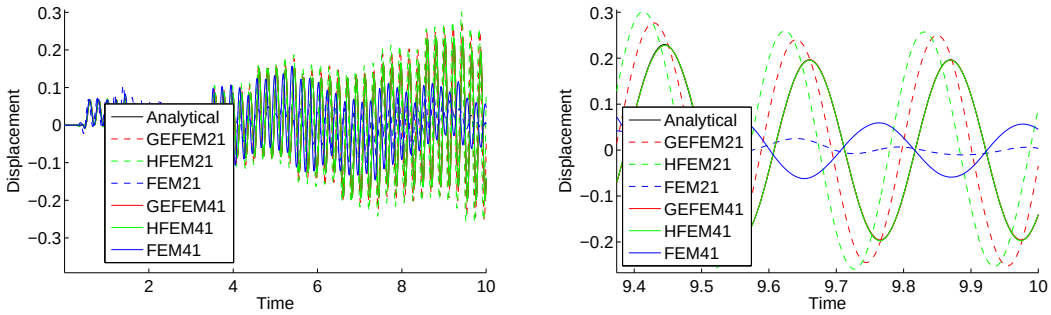

Figure 13: Analytical and numerical results for $\omega = 30$ at the middle of the bar for the second example.

From these results it can be seen that both the GFEM and the HFEM presented better results than the FEM with linear elements. In Fig. 12 the solutions given by the GFEM and the HFEM are almost identical to the analytical solution, while the solution given by the FEM with linear elements is not as accurate as the other two. In Fig. 13 the solutions given by the GFEM and the HFEM for 41 degrees of freedom are also almost identical to the analytical solution, while the solutions given by the FEM are very poor.

The errors presented in Tab. 2 and Tab. 3 also show that the results by the GFEM and by the HFEM are much better than the one given by the FEM using linear elements. It is also interesting to note that the errors given by the FEM for both 21 and 41 degrees of freedom are almost the same. This indicates that the FEM is not able to reproduce the analytical solution adequately. Finally, the GFEM presented better results than the HFEM for this example.

Error	GFEM21	HFEM21	FEM21	GFEM41	HFEM41	FEM41
e_p	6.6275e-004	8.1969e-004	2.5703e-002	1.4103e-004	1.5886e-004	6.8325e-003
e_g	6.7929e-003	8.1286e-003	2.6448e-001	1.3957e-003	1.5899e-003	7.1470e-002

Table 2: Errors for the second example for $\omega = 10$.

Error	GFEM21	HFEM21	FEM21	GFEM41	HFEM41	FEM41
e_p	2.5999e-002	4.7577e-002	8.7083e-002	4.7481e-004	4.9143e-004	1.0390e-001
e_g	3.1942e-001	5.6963e-001	8.2445e-001	5.7397e-003	5.8875e-003	9.4303e-001

Table 3: Errors for the second example for $\omega = 30$.

6.3 Third example: truss subjected to an harmonic force

The third and last example is that of the truss from Fig. 14, that is subjected to an harmonic force and null initial displacements. This is an interesting example since it is not possible to increase the number of degrees of freedom when using the FEM with linear elements. That's because each bar cannot be divided in two finite elements since this would create a mechanism inside the structure. When using the GFEM and the HFEM, instead, its is possible to increase the number of degrees of freedom by increasing the number of shape functions.

Here we assume that the applied force show in Fig. 14 has a frequency $\omega = 5$ and a magnitude $f = 1$. All bars have $E = 1$, $A = 1$ and $\rho = 1$. The length L shown in Fig. 14 is also taken equal to 1. Finally, the time step is taken equal to $\Delta t = 0.0125$.

This problem is solved using the FEM with linear elements, using the GFEM and using the HFEM. For both the GFEM and the HFEM two cases are studied, using 4 enrichment functions and using 8 enrichment functions. The extra shape functions needed for the GFEM can be obtained by assuming $i = 1, 2, ..., n$ in Eq. (6). For the HFEM, instead, generation of the extra shape functions is not an easy task. However, Lobatto polynomials up to order 10 are presented by Solín et al. (2004).

The vertical displacement of the node shown in Fig. 14 is presented in Fig. 15, where the number after the name of the formulation indicates the number of enrichment functions used. The results given by the GFEM and the HFEM appear to converge to the same result. The results given by the FEM with linear elements, instead, do not agree with those give by the the GFEM and the HFEM.

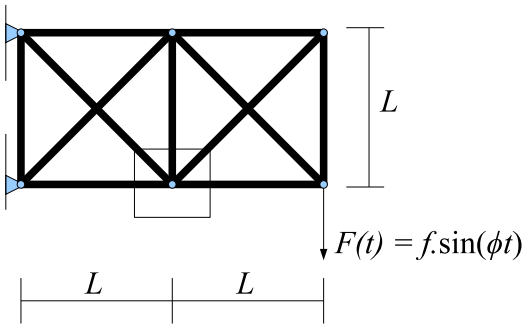

Figure 14: Truss subjected to an harmonic force.

As discussed previously, when using the FEM formulation it is not possible to increase the number of degrees of freedom used. Consequently, one cannot improve accuracy of the results

for a fixed time step. When using the GFEM and the HFEM, instead, accuracy can be improved by increasing the number of enrichment functions.

The results given both by the GFEM and the HFEM seem to converge to the same solution. The results given by the FEM, however, do note agree with the results given by the GFEM and the HFEM. This is an evidence that the results given by the FEM with linear elements are unsatisfactory for this example. Another evidence of this statement can be found in Fig. 15, for the time interval [0,1]. When using the GFEM and the HFEM the motion only arrives at the node considered after some time. This is an expected behavior, since the motion really takes some time to exert its influence over all parts of the structure. However, when using the FEM with linear elements, the motion is "felt" at the node considered almost instantaneously. This, appears to put in evidence the inability of the standard FEM to reproduce the wave propagation phenomenon.

Errors estimates for this example cannot be evaluated, since the analytical solution of this problem is not known. Anyway, it seems that both the GFEM and the HFEM performed better than the FEM in this case. However, it is important to point out that the generation of extra enrichment functions for the HFEM are not an easy task, and in most cases one is limited to the Lobatto polynomials presented in literature. The extra enrichment functions used by the GFEM, instead, can be readily obtained by assuming $i = 1, 2, ...$ in Eq. (6).

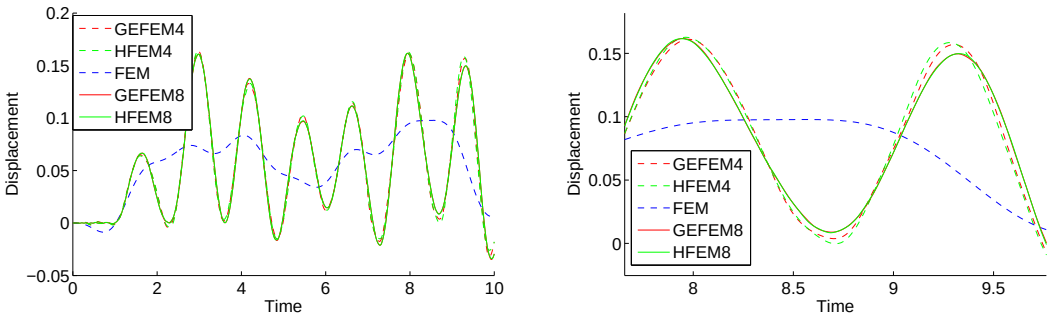

Figure 15: Vertical displacement of the node shown in Fig. 14.

7 CONCLUSIONS

This paper presented a GFEM formulation for the transient dynamic analysis of bars and trusses. The time integration procedure was implemented using the Newmark method. Numerical errors can result both from the time integration procedure and from the finite element model. Errors from the numerical integration procedure can be reduced by decreasing the time step used, while errors from the finite element model can be reduced by using a more accurate approximation.

The GFEM allows one to use an enriched approximation for the displacements that is easy to obtain and does not affect nodal quantities. This approximation leads to better results than standard linear FEM. For the wave propagation phenomenon the GFEM also gives results at least as good as classical HFEM using Lobatto polynomials. Besides, this GFEM formulation is an hierarchical one (as is the case of HFEM), since the approximation can be enriched without changing the shape functions already used.

The GFEM approach proposed here can be applied to both dynamic analysis problems and wave propagation problems. Notice that a FEM formulation with linear elements is inappropriate for most wave propagation problems, since one would needs too many degrees of freedom

in order to capture an accurate result. This is especially true for problems involving truss structures, since the division of bars in more that one element leads to computational difficulties.

REFERENCES

Ardnt M., Machado R., and Scremin A. An adaptive generalized finite element method applied to free vibration analysis of straight bars and trusses. *Journal of Sound and Vibration*, 329:659–672, 2010.

Arndt M. *O Método dos Elementos Finitos Generalizados Aplicados à Análise de Vibrações Livres de Estruturas Reticuladas*. Ph.D. thesis, Universidade Federal do Paraná, Brasil, 2009.

Babuska I., Banerjee U., and Osborn J. Generalized finite element methods: main ideas, results, and perspective. *TICAM Technical Report*, (04-08), 2004.

Bathe K. *Finite Element Procedures*. Prentice Hall, Upper Saddle River, 1996.

Chopra A. *Dynamics of Structures: Theory and applications to earthquake engineering*. Prentice Hall, 1995.

Hughes T. *The Finite Element Method: Linear Static and Dynamic Finite Element Analysis*. Dover Publications, 2000.

Kreyszig E. *Introductory Functional Analysis with Applications*. John Wiley & Sons, 1978.

Kreyszig E. *Advanced Engineering Mathematics*. John Wiley & Sons, 9 edition, 2006.

Melenk J. and Babuska I. The partition of unity finite element method: Basic theory and applications. *Computer Methods in Applied Mechanics and Engineering*, 139(1-4):289–314, 1996.

Pinchover Y. and Rubinstein J. *An Introduction to Partial Differential Equations*. Cambridge University Press, Cambridge, 2005.

Reddy B. *Introductory Functional Analysis: With Applications to Boundary Value Problems and Finite Elements*, volume 27 of *Texts in Applied Mathematics*. Springer-Verlag, New York, 1998.

Solín P., Segeth K., and Dolezel I. *Higher-order finite element methods*. Studies in Advanced Mathematics. Chapman & Hall-CRC, Boca Raton, 2004.

Strouboulis T., Copps K., and Babuska I. The generalized finite element method. *Computer Methods in Applied Mechanics and Engineering*, 190:4081–4193, 2001.

Zienkiewicz O. and Taylor R. *The finite element method*, volume II. McGraw Hill, 1991.